Pharmaceutical Research, Vol. 9, No. 2, 1992

Research Article

Pharmacokinetic Analysis of Drug Absorption from Muscle Based on a Physiological Diffusion Model: Effect of Molecular Size on Absorption

Eiji Nara,[1] Masaaki Masegi,[1] Tetsuya Hatono,[1] and Mitsuru Hashida[1,2]

Received June 3, 1991; accepted September 1, 1991

In a rabbit hind leg perfusion experiment, the absorption of radiolabeled water and carbohydrates of various molecular sizes from muscle was analyzed using a physiological diffusion model and, also, by statistical moment analysis. The model takes into account diffusion in the interstitial space, transcapillary movement, and removal by the blood circulation and pharmacokinetic parameters representing these processes were computed by curve-fitting. The apparent diffusion coefficients of water and small sugars in the interstitial space (D_m) were proportional to their free diffusion coefficients in water (D_f), whereas the diffusion of ^{14}C-inulin was hampered by interstitial structures. The first moments of each absorption process were also determined to assess the quantitative contribution of each absorption process to overall absorption. For carbohydrate molecules, residence time in the depot ($\bar{t}_d$) accounted for most of the absorption time after injection, whereas for ^{3}H-water, residence times in muscle ($\bar{t}_m$) and in the depot ($\bar{t}_d$) were similar.

KEY WORDS: intramuscular injection; absorption; physiological diffusion model; statistical moments; rabbit hind leg perfusion; molecular size.

INTRODUCTION

The absorption of drugs after intramuscular (*im*) injection has been thoroughly studied. Various physicochemical and physiological factors are known to influence drug absorption from muscle (1,2), but the mechanism is not well understood. The absorption of *im* injected drugs depends on tissue structure, capillary construction, and local blood flow. Pharmacokinetic studies of absorption have been published (3–5), but a quantitative description of absorption is not available.

We have previously reported a new method to assess drug absorption from muscle in a rabbit hind leg perfusion system, by statistical moment analysis of ^{14}C-sucrose (6). We now introduce a new pharmacokinetic model which takes the following three processes into consideration: (a) diffusion in the interstitial space, (b) permeation across the capillary wall, and (c) removal by the local perfusion.

The Laplace transforms of the mass-balance equations describing drug absorption rate were derived from this model and fitted to venous appearance curves after *im* injection with the aid of MULTI(FILT), a nonlinear least-squares regression computer program based on a fast inverse Laplace transform algorithm (7). Radiolabeled water, mannitol, sucrose, and inulin were chosen as model compounds, and the effect of molecular size on drug absorption from muscle was examined. The overall absorption was also evaluated by statistical moment analysis.

THEORETICAL

A Model of Drug Absorption from Muscle

In the model shown in Fig. 1, drug molecules are assumed to arrive at the sampling point in the following way: the injected drug solution forms a depot in the interstitial space with a volume equal to the injection volume (100 μl). The interstitial space is assumed to be an infinitely large homogeneous plane layer, and drug molecules diffuse along a unidirectional concentration gradient, away from the injection depot. At any distance from the depot, drug molecules can move to blood vessels or intracellular space. Blood vessels are arranged continuously along the muscle and their flow direction is perpendicular to the diffusion direction. Drug molecules which permeate the capillary wall are transported to the sampling point by local flow. In the models, well-stirred conditions are assumed to exist both in the injection depot and in each blood vessel. In the interstitial space, well-stirred concentrations are also assumed to exist on the plane vertical to the diffusion direction.

Analysis of the Venous Appearance Curve of ^{3}H-Water

Because water molecules permeate both capillary walls and cell membranes quickly (8), no concentration gradient is

[1] Department of Basic Pharmaceutics, Faculty of Pharmaceutical Sciences, Kyoto University, Sakyo-ku, Kyoto 606, Japan.

[2] To whom correspondence should be addressed at Faculty of Pharmaceutical Sciences, Kyoto University, Sakyo-ku, Kyoto, 606, Japan.

0724-8741/92/0200-0161$06.50/0

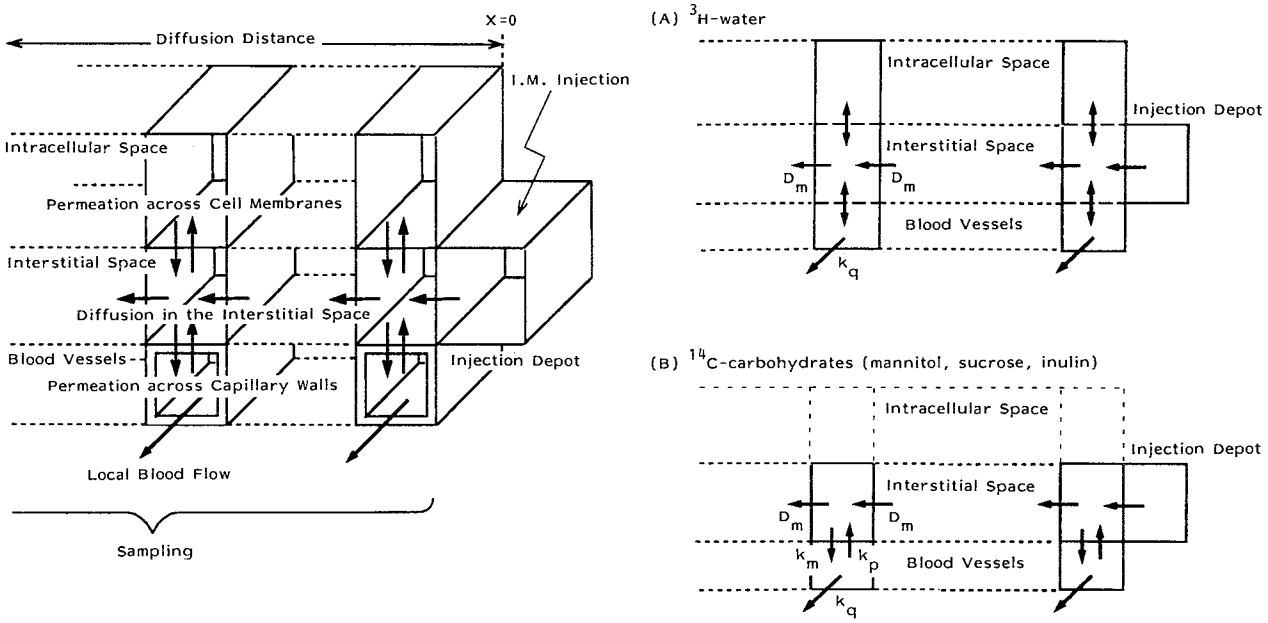

Fig. 1. The physiological diffusion model used for the analysis of venous appearance curves. (A) ^{3}H-Water; (B) ^{14}C-labeled carbohydrates. D_m, apparent diffusion coefficient; k_m, permeation rate constant from interstitial side; k_p, permeation rate constant from vascular side; k_q, perfusion rate constant.

assumed to exist across either membrane. Therefore, the model used to analyze ^{3}H-water absorption is approximated as shown in Fig. 1A. Water molecules diffuse in the interstitial space with an apparent diffusion coefficient D_m and are transported to the sampling point by local flow. Then the following differential equation can be constructed for the ^{3}H-water in muscle at a distance X from the surface of the depot at time t.

$$\frac{\partial C_m}{\partial t} = D_m r_i \frac{\partial^2 C_m}{\partial X^2} - k_q r_p C_m \tag{1}$$

where C_m is the concentration of ^{3}H-water in muscle and k_q is the vascular perfusion rate constant (local perfusion rate per unit vascular volume). r_p and r_i are the volume of vascular space and interstitial space, respectively, as a fraction of the total water space. A is an apparent diffusion area (the volume per unit length for the interstitial space), which is assumed to be constant throughout diffusion. The boundary and initial conditions are as follows (X_0, injected dose);

$$C_m = C_d \qquad (X = 0) \tag{2}$$

$$V_d \frac{\partial C_d}{\partial t} = D_m A \frac{\partial C_m}{\partial X} \qquad (X = 0) \tag{3}$$

$$\frac{\partial C_m}{\partial X} = 0 \qquad (X = \infty) \tag{4}$$

$$V_d C_d = X_0 \qquad (t = 0) \tag{5}$$

$$C_m = 0 \qquad (t = 0) \tag{6}$$

where C_d is the concentration of ^{3}H-water in the depot and V_d is the volume of the depot. The Laplace transforms of the equations of the absorption rate ($\bar{J}_a$) and the amounts remaining in the depot ($\bar{M}_d$) and in muscle ($\bar{M}_m$) are as follows, respectively (see Appendix A):

$$\bar{J}_a = \frac{k_q r_p X_0}{aq(s) + sV_d[r_i aq(s)]^{1/2}/da} \tag{7}$$

$$\bar{M}_d = \frac{X_0 V_d}{sV_d + da[aq(s)/r_i]^{1/2}} \tag{8}$$

$$\bar{M}_m = \frac{X_0 da(r_i + r_c)}{sV_d[r_i aq(s)]^{1/2} + daaq(s)} \tag{9}$$

where s is the Laplace variable with respect to time and r_c is the volume of the intracellular space as a fraction of the total water space. da is a hybrid diffusion parameter including A as follows:

$$da = D_m^{1/2} A \tag{10}$$

$$aq(s) = s + r_p k_q \tag{11}$$

Local flow rate (Q_p) is derived from k_q and the volume of the vascular space (V_p) as follows:

$$Q_p = k_q V_p \tag{12}$$

Analysis of the Venous Appearance Curves of ^{14}C-Labeled Carbohydrates

^{14}C-Labeled carbohydrates used in this study distribute only in the interstitial space (9), and they permeate capillary walls by passive diffusion. The model for the venous appearance curves of these carbohydrates is approximated as shown in Fig. 1B. The following mass balance equations for these compounds in the interstitial space and perfusate are given at a distance X from the surface of the injection depot at time t.

$$\frac{\partial C_m}{\partial t} = D_m \frac{\partial^2 C_m}{\partial X^2} - k_m C_m + k_p(r_p/r_i)C_p \quad (13)$$

$$\frac{\partial C_p}{\partial t} = k_m(r_i/r_p)C_m - (k_p + k_q)C_p \quad (14)$$

where C_p and C_m are the concentrations of carbohydrate in the perfusate and in the interstitial space, respectively. k_m and k_p are the permeation rate constants at the capillary wall from the interstitial and vascular sides, respectively. The initial and boundary conditions are as follows:

$$C_m = C_d \quad (X = 0) \quad (15)$$

$$V_d \frac{\partial C_d}{\partial t} = D_m A \frac{\partial C_m}{\partial X} \quad (X = 0) \quad (16)$$

$$\frac{\partial C_m}{\partial X} = 0 \quad (X = \infty) \quad (17)$$

$$V_d C_d = X_0 \quad (t = 0) \quad (18)$$

$$C_m = 0 \quad (t = 0) \quad (19)$$

The Laplace-transformed equations of absorption rate ($\bar{J}_a$) and the amounts remaining in the depot ($\bar{M}_d$) and in muscle ($\bar{M}_m$) are (see Appendix A):

$$\bar{J}_a = \frac{k_m k_q da X_0}{sV_d[(s + k_p + k_q)bq(s)]^{1/2} + dabq(s)} \quad (20)$$

$$\bar{M}_d = \frac{V_d(s + k_p + k_q)^{1/2} X_0}{sV_d(s + k_p + k_q)^{1/2} + dabq(s)^{1/2}} \quad (21)$$

$$\bar{M}_m = \frac{da(s + k_p + k_q)X_0}{sV_d[(s + k_p + k_q)bq(s)]^{1/2} + dabq(s)} \quad (22)$$

where

$$bq(s) = s^2 + (k_m + k_p + k_q)\, s + k_m k_q \quad (23)$$

Since carbohydrate permeate the capillary wall by passive diffusion, the following relation is valid and vascular permeation clearance (CL_p) is derived from k_p and from the volume of the vascular space as follows:

$$k_p = (r_i/r_p)k_m \quad (24)$$

$$CL_p = k_p V_p \quad (25)$$

First Moments for Each Absorption Process

Mean arrival time ($\bar{t}_a$) for ^{3}H-water is derived as (see Appendix B)

$$\bar{t}_a = \frac{1}{r_p k_q} + \left(\frac{r_i}{r_p k_q}\right)^{1/2} \frac{V_d}{da} \quad (26)$$

First moments for each absorption process (Fig. 2A) are calculated as follows (see Appendix B):

$$\bar{t}_d = \left(\frac{r_i}{r_p k_q}\right)^{1/2} \frac{V_d}{da} \quad (27)$$

$$\bar{t}_m = \left(\frac{r_i + r_c}{r_p}\right) \frac{1}{k_q} \quad (28)$$

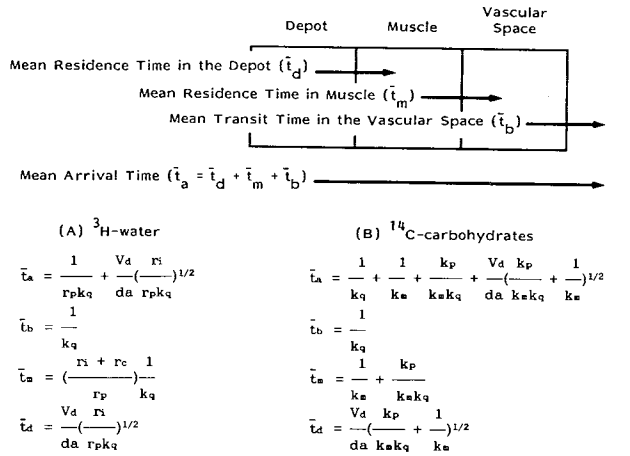

Fig. 2. First moments for absorption processes of *im* injected drug. (A) ^{3}H-Water; (B) ^{14}C-labeled carbohydrate.

$$\bar{t}_b = \frac{1}{k_q} \quad (29)$$

In the case of ^{14}C-labeled carbohydrates (Fig. 2B), $\bar{t}_a$ and the first moments for each absorption process are (See Appendix B)

$$\bar{t}_a = \frac{1}{k_q} + \frac{1}{k_m} + \frac{k_p}{k_m k_q} + \frac{V_d}{da}\left(\frac{k_p}{k_m k_q} + \frac{1}{k_m}\right)^{1/2} \quad (30)$$

$$\bar{t}_d = \frac{V_d}{da}\left(\frac{1}{k_m} + \frac{k_p}{k_m k_q}\right)^{1/2} \quad (31)$$

$$\bar{t}_m = \frac{1}{k_m} + \frac{k_p}{k_m k_q} \quad (32)$$

$$\bar{t}_b = \frac{1}{k_q} \quad (33)$$

EXPERIMENTAL

Animals

Male rabbits (1.8–2.1 kg) with free access to a commercial diet and waters were used.

Materials

^{3}H-Water, D-[1-^{14}C]mannitol, [^{14}C(U)]sucrose, and [methoxy-^{14}C]inulin were purchased from New England Nuclear, Boston, MA. Indium chloride-111 ([^{111}In]$InCl_3$) was kindly supplied by Nihon Medi-Physics, Co., Takarazuka, Japan. Bovine serum albumin (BSA; fraction V) and all other chemicals of reagent grade were obtained commercially from Nacalai Tesque Inc., Kyoto, Japan. BSA was labeled with ^{111}In with the bifunctional chelating agent diethylenetriaminepentaacetic acid (DTPA) anhydride according to the method of Hnatowich *et al.* with slight modification (10).

Absorption from Perfused Rabbit Muscle

Absorption experiments were performed as described previously (6). The right legs of anesthetized rabbits were perfused at 1.7 ml/min. The perfusion medium was Tyrode's solution with BSA (5%, w/v), which was oxygenated with

95% O_2–5% CO_2 to pH 7.4 at 37°C. After the animal was given a lethal intravenous injection of aqueous pentobarbital, phosphate buffer solution (100 μl, pH 7.4) containing radiolabeled compounds was injected over 40 sec into the center of the *musclus gastrocnemius* at a depth of 8 mm. Twenty seconds after the injection sampling began and the venous effluent was collected for 120 min. The injection point was covered with surgical adhesive to prevent fluid leakage.

Assay

The radioactivities of ^3H and ^{14}C in the supernatant of the effluents were measured with a liquid scintillation counter (LSC-900, Aloka Co., Tokyo) after centrifugation (3000 rpm × 5 min). The radioactivity of ^{111}In in the outflow was counted with a gamma counter (ARC-500, Aloka Co., Tokyo).

Determination of Intravascular, Extracellular, and Intracellular Volumes

Indicator dilution experiments were performed using ^{111}In-BSA, ^{14}C-sucrose, and ^3H-water as reference substances to determine the volumes of the vascular, extracellular, and intracellular spaces, respectively. Details of the procedures were reported previously (11). Marker substances dissolved in the perfusate (0.103 ml) were introduced into the femoral artery using a six-position rotary valve injector (Type 50 Teflon Rotary Valves, Rheodyne, CA) as a pulse function. The venous effluent was collected at appropriate intervals (first 5 sec, then 1–6 min) for 30 min (for BSA) or 60 min (for sucrose and water).

Data were analyzed based on statistical moment theory. The mean transit time ($\bar{t}_i$) for each marker substance was defined as (11)

$$\bar{t}_i = \int_0^\infty tCdt \Big/ \int_0^\infty Cdt \tag{34}$$

where t is the sampling time, and C is the concentration of each substance normalized by injection dose as a percentage of the dose per milliliter. For noneliminated substances, the distribution volume (V_i) was defined in terms of organ perfusion rate (Q) and $\bar{t}_i$ for the substance by (12)

$$V_i = \bar{t}_i Q \tag{35}$$

The $\bar{t}_i$ values were calculated by numerical integration using a linear trapezoidal formula and extrapolation to infinite time based on a monoexponential equation. The $\bar{t}_i$ values were corrected for the lag time of the catheter.

Calculation of Statistical Moments for Venous Appearance Curves

The first three moments for the venous appearance curves are defined as follows (6):

$$F_a = \int_0^\infty Jdt \tag{36}$$

$$\bar{t}_a = \int_0^\infty tJdt/F_a \tag{37}$$

$$\sigma_a^2 = \int_0^\infty (t - \bar{t}_a)^2 Jdt/F_a \tag{38}$$

where t is the sampling time and J is the absorption rate of each compound normalized by the injected dose as a percentage of the dose per minute. F_a, $\bar{t}_a$, and σ_a^2 are the fraction absorbed, the mean arrival time to the venous sampling point, and the variance of the arrival time, respectively. The moments were calculated as described above. The $\bar{t}_a$ and σ_a^2 values were not corrected for the lag time of the catheter or its variation.

Analysis of Venous Appearance Curves Based on a Physiological Diffusion Model

First, r_p, r_i, and r_c were estimated by the indicator dilution experiments. Then Eq. (7), in which the estimated values had been substituted for r_p and r_i, was fitted to the mean venous appearance curve of ^3H-water with MULTI (FILT), and the da (for water) and k_q values were determined. This nonlinear regression program is written in FORTRAN 77 and developed on the main computer M-382 of the Kyoto University Data Processing Center. Next da and k_m were determined for each ^{14}C-labeled carbohydrate by the curve-fitting of Eq. (22), after the values of k_q, r_p, and r_i had been substituted in, to the mean appearance curves. Finally, Q_p, k_p, and CLp were calculated using Eqs. (12), (24), and (25), respectively.

RESULTS

Intravascular, Interstitial, and Intracellular Volumes

Figure 3 shows typical dilution curves of marker substances. The dilution curve of ^{14}C-sucrose had a lower peak concentration than that of ^{111}In-BSA. The ^3H-water peak was lowest, reflecting its larger distribution volume. The calculated t_i and V_i values for these substances are summarized in Table I. The recovery ratios were almost 100% in all cases (data not shown). The volumes of the vascular and extracellular spaces were 3.70 and 22.30 ml/100 g muscle, respectively, which are in good agreement with the values reported previously (11,13). The volume of total water space in muscle was 75.8 ml/100 g muscle, which is comparable to the value of muscle water content in the perfused limbs, 75.9%

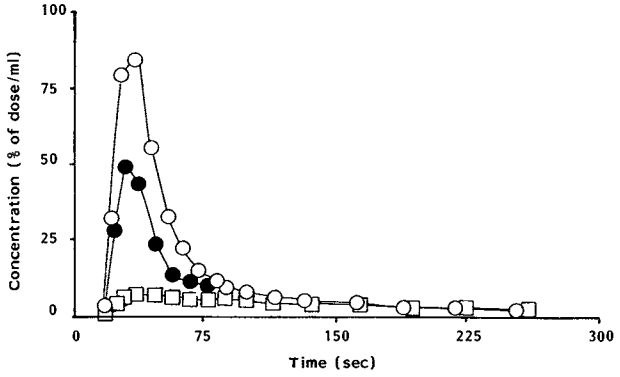

Fig. 3. Typical dilution curves of ^{111}In-BSA (○), ^{14}C-sucrose (●), and ^3H-water (□) after bolus injection into the rabbit femoral artery.

Table I. Mean Transit Times and Volumes of Distribution for Marker Substances After Bolus Injection into the Femoral Artery[a]

Compound	$\bar{t}_i$ (min)	V_i^b (ml/100 g muscle)
^{111}In-BSA	1.09 ± 0.04	3.70 ± 0.19
^{14}C-Sucrose	6.67 ± 0.57	22.30 ± 1.32
^{3}H-Water	22.65 ± 1.11	75.82 ± 4.00

[a] Values are means ± SD.
[b] This value was estimated assuming that the perfused muscle weight was 51.4 g (11).

Table II. Values of Moment Parameters for Absorption of *im* Injected Test Compounds in the Perfusion Experiment[a]

Compound	F_a (% dose)	$\bar{t}_a$ (min)	σ_a^2 (min^2)
^{3}H-Water	103.5 ± 4.5	49.2 ± 5.1	1,819 ± 398
^{14}C-Mannitol	103.1 ± 3.5	45.5 ± 8.0	1,483 ± 598
^{14}C-Sucrose[b]	104.0 ± 5.3	50.5 ± 4.0	1,983 ± 326
^{14}C-Inulin	112.0 ± 24.4	215.1 ± 57.7	45,270 ± 21,263

[a] Values are means ± SD.
[b] These data were taken from Ref. 6.

of wet weight. From these values, volumes of interstitial and intracellular space were determined to be 18.6 and 53.5 ml/100 g muscle, respectively.

Venous Appearance Curves of ^{3}H-Water and ^{14}C-Labeled Carbohydrates After *im* Injection

The mean venous appearance curves for the test compounds are shown in Fig. 4. The absorption rate of ^{3}H-water reached a peak about 15 min after the injection and then fell off in a nearly monoexponential fashion. In comparison, the absorption rate of ^{14}C-inulin reached a lower peak and then decreased more slowly. The venous appearance curves of the other two carbohydrates were similar to that of ^{3}H-water.

Statistical Moment Analysis of Venous Appearance Curves

Moment parameters calculated from venous appearance curves are summarized in Table II. The F_a and $\bar{t}_a$ values for ^{3}H-water were 103.5% and 49.2 min, respectively. The $\bar{t}_a$ values for ^{14}C-mannitol, ^{14}C-sucrose, and ^{14}C-inulin were 45.5, 50.5, and 215.1 min, respectively. Thus, the absorption rates of the carbohydrates were inversely related to molecular size. On the other hand, the $\bar{t}_a$ value for ^{3}H-water was similar to those of ^{14}C-mannitol and ^{14}C-sucrose, reflecting their distribution characteristics.

Analysis of Venous Appearance Curves Based on a Physiological Diffusion Model

The values of the parameters obtained by model analysis are listed in Table III. In this model analysis, values of many unknown parameters are required to describe absorption. However, three of them (r_p, r_i, and r_c) can be obtained preliminarily and only two parameters were estimated by curve-fitting to one data set. Thus the estimated values shown in Table III seem to be reasonable. Since the average weight of perfused muscle in this system is reported to be

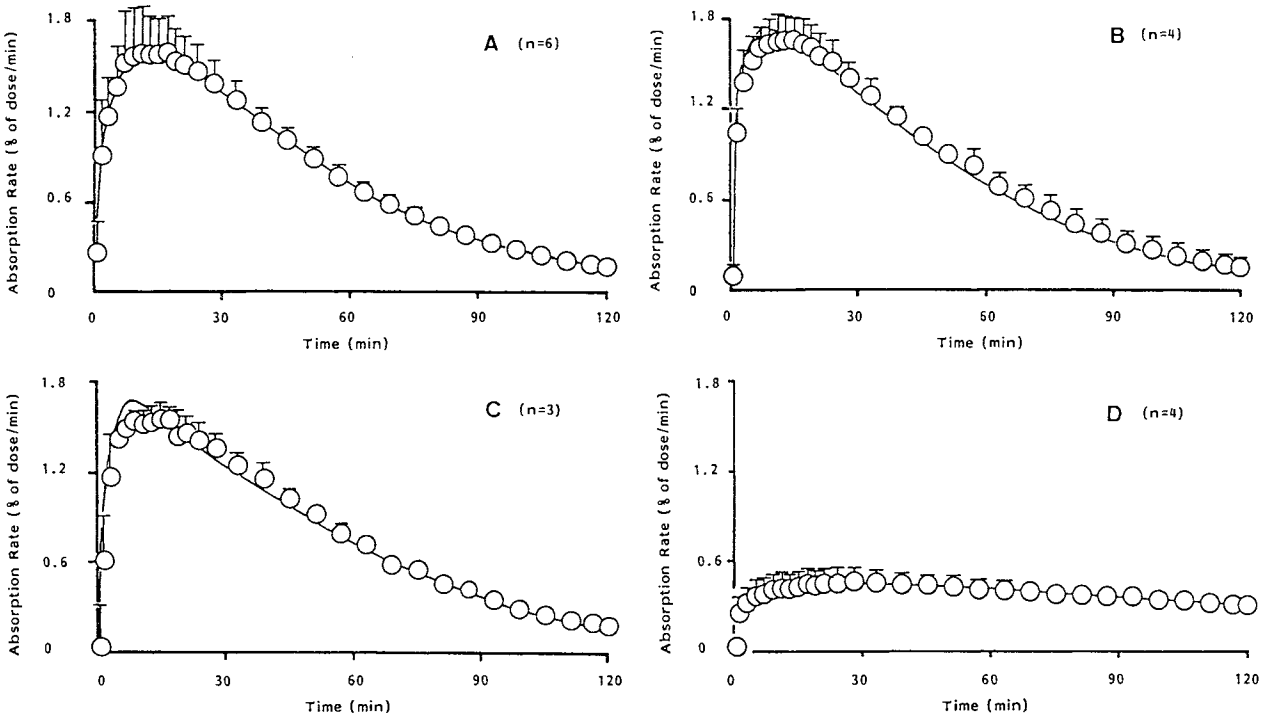

Fig. 4. Venous appearance curves of ^{3}H-water (A), ^{14}C-mannitol (B), ^{14}C-sucrose (C), and ^{14}C-inulin (D) after *im* injection. The results are expressed as the means of at least three experiments (numbers in parentheses represent the number of experiments) and the vertical bars indicate standard deviations. The solid lines were calculated using the parameters listed in Table III.

Table III. Estimated Values of Parameters for the Absorption of *im* Injected Test Compounds in the Perfusion Experiment

Compound	da (ml/min$^{1/2}$)	k_q (min^{-1})	Q_p[a] (ml/min/100 g)	k_m (min^{-1})	k_p (min^{-1})	CL_p[a] (ml/min/100 g)
^{3}H-Water	0.00804	1.02	3.77	—	—	—
^{14}C-Mannitol	0.00515	(1.02)	(3.77)	7.06	35.6	131.4
^{14}C-Sucrose	0.00465	(1.02)	(3.77)	5.36	27.0	99.7
^{14}C-Inulin	0.00121	(1.02)	(3.77)	1.46	7.37	27.2

[a] This value was estimated assuming that the perfused muscle weight was 51.4 g (11).

51.4 g (11), Q_p was calculated to be 3.78 ml/min/100 g muscle, which is close to the set flow rate of the perfusate (3.31 ml/min/100 g muscle). Estimated *da* values were lower for larger injected compounds. While *da* is determined as a hybrid parameter including *A*, *A* is assumed to be constant in this study. Therefore, the *da* values are believed to indicate directly the diffusivity of test compounds. CL_p was also lower for larger carbohydrate, but it was much larger than Q_p.

First Moments for Each Absorption Process

The mean time values for each absorption process (first moments) of model compounds are shown in Fig. 5. The $\bar{t}_a$ values obtained by curve-fitting were in good agreement with those obtained directly from moment analysis. In the case of carbohydrates, the contributions of $\bar{t}_b$ and $\bar{t}_m$ to the total $\bar{t}_a$ were small. On the other hand, $\bar{t}_m$ of ^{3}H-water was comparable to $\bar{t}_d$.

DISCUSSION

We used a perfused rabbit hind leg to study drug absorption from muscle. Using this system, we can obtain direct and detailed information on drug absorption from venous appearance curves, which is valuable for understanding the mechanism of absorption. Absorption of carbohydrates of different molecular sizes was examined together with an absorption of ^{3}H-water, using both statistical moment analysis and a pharmacokinetic model.

The values of the parameters obtained from statistical moment analysis are free from the complexities of a pharmacokinetic model and the overall absorption process can be evaluated stochastically with respect to rate and extent (6). F_a values for test compounds were almost 100%, which indicates, complete absorption of these compounds from muscle. On the other hand, the $\bar{t}_a$ value was directly related to the molecular size of the injected carbohydrate, suggesting that molecular size is a important determinant of the rate of absorption from muscle. Similar findings have been reported for drug absorption from both muscle and subcutaneous tissue (1,2). However, moment analysis does not allow analysis of total absorption into the contributions of various absorption processes. Moreover, this analysis can be applied only to drugs which are absorbed relatively rapidly. When the absorption fraction is still small at the end of the experiment, much of the fraction must be estimated by extrapolation of the slope of the terminal phase, which entails a relatively large error.

In contrast, a pharmacokinetic model allows analysis of absorption into its component processes. The model used in this study represents three physicochemical and physiological processes (diffusion in the interstitial space, movement across the capillary wall, and removal by the local perfusion) and allows us to understand absorption with parameters reflecting each of these processes.

Since heterogeneity of blood flow has been reported to exist in skeletal muscle (14,15), the local perfusion rate of the injection site may not be equal to the overall perfusion rate set by the peristaltic roller pump. In this study, the local perfusion rate (Q_p) is estimated from curve-fitting of the venous appearance curve of ^{3}H-water, but the estimated Q_p value is comparable to the set average perfusion rate.

The D_m ratio of each model compound to ^{14}C-sucrose was calculated from the *da* value assuming that *A* is constant and is plotted against molecular radius, together with its D_f (free diffusion coefficient in water, 37°C) ratio to sucrose, in Fig. 6. The D_m ratios for model compounds smaller than

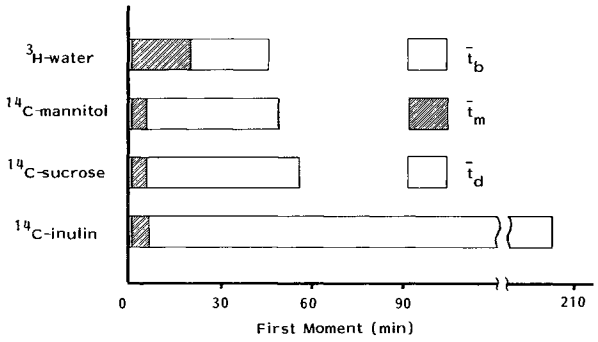

Fig. 5. First moments for model compounds after *im* injection. These values were calculated using the equations in Figs. 2A and B, with the values of the parameters listed in Table III.

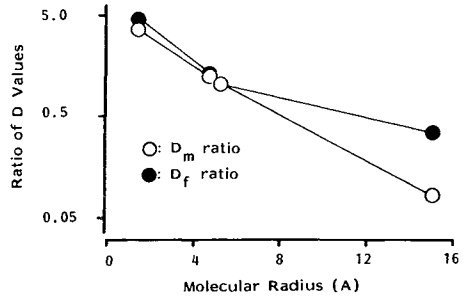

Fig. 6. The relationship between D_m and D_f ratios and molecular radius. The ratios of D_m and D_f of each compound to those of sucrose are plotted against molecular radius. The D_m ratios were calculated from *da* values listed in Table III, and D_f values are taken from published data (8).

sucrose were closes to their D_f ratios. However, the D_m ratio of inulin is much smaller than its D_f ratio, which shows that the diffusion of inulin is restricted in the interstitial space. Restricted diffusive transport of macromolecules in the interstitial space has been explained by the steric hindrance between solute and interstitial matrix (16,17). In addition, hyaluronidase, which destroys the hyaluronate gel formation in the interstitial connective tissue, was reported to have a greater effect on the absorption of inulin than on the absorption of smaller molecules (18,19). The present analysis, based on a physiological diffusion model, demonstrates that, in theory, the interstitial diffusion of inulin should be reduced and this analysis may further explain the previous findings regarding the effect of hyaluronidase.

The movement of hydrophilic molecules across the capillary wall is believed to be limited to small pores filled with water. This route of transport is hindered by steric interaction between the molecules and the pore walls, and the extent of this restriction is determined by the balance of their sizes (8). In this study, estimated CL_p values for ^{14}C-labeled carbohydrates were lower for larger molecules, but CL_p values were reduced more than D_f values, suggesting that the passage of these carbohydrates is restricted by steric interaction.

da, CL_p, and Q_p are the basic parameters used to describe absorption of drugs, and their balance determines the rate of each absorption step and the total absorption. The first moment of each absorption process indicates the contribution of that process to the overall absorption (20). In the present study, first moments are given separately for the processes which traverse the boundaries between neighboring layers (Figs. 2A and B). Carbohydrate molecules remained in the depot for most of the time required for their total absorption after *im* injection, and the rate-limiting step was the movement from the depot to the muscle (Fig. 6). In the case of ^3H-water, however, $\bar{t}_m$ was almost equal to $\bar{t}_d$. This difference in absorption arises from the difference in their diffusibility and distribution in muscle. Since the distribution of carbohydrates is restricted to the extracellular space, the time required to wash out the space by local perfusion is short. However, their relatively slow diffusion in the interstitial space means that removal of injected molecules from the depot is slow. In the case of ^3H-water, a long time is required to wash out its large distribution volume. However, the diffusive transport of ^3H-water is rather rapid, which results in a comparatively fast removal of injected solute. Consequently, although the time necessary for complete absorption ($\bar{t}_a$) of ^3H-water is similar to that required for complete absorption of ^{14}C-mannitol and ^{14}C-sucrose, the contribution of each absorption process is rather different.

APPENDIX A: LAPLACE-TRANSFORMED EQUATIONS FOR THE PHYSIOLOGICAL DIFFUSION MODELS (FIG. 1)

For ^3H-water, the Laplace transforms of Eqs. (1)–(4) are, respectively,

$$s\overline{C}_m = D_m r_i \frac{\partial^2 \overline{C}_m}{\partial X^2} - k_q r_p \overline{C}_m \tag{A1}$$

$$\overline{C}_m = \overline{C}_d \qquad (X = 0) \tag{A2}$$

$$sV_d\overline{C}_d = D_m A \frac{\partial \overline{C}_m}{\partial X} + X_0 \qquad (X = 0) \tag{A3}$$

$$\frac{\partial \overline{C}_m}{\partial X} = 0 \qquad (X = \infty) \tag{A4}$$

Equation (A1) has the general solutions

$$\overline{C}_m = A' \exp(-q_m X) + B' \exp(q_m X) \tag{A5}$$

where

$$q_m = [(s + k_q r_p)/(D_m r_i)]^{1/2} \tag{A6}$$

From Eqs. (A2)–(A6), A' and B' are determined, respectively, as

$$A' = X_0/(sV_d + D_m A q_m) \tag{A7}$$

$$B' = 0 \tag{A8}$$

$\bar{J}_a$, $\overline{M}_d$ and $\overline{M}_m$ are calculated, respectively, by

$$\bar{J}_a = \int_0^\infty k_q A' \overline{C}_p \partial X = \frac{k_q A' X_0}{q_m(sV_d + D_m A q_m)} \tag{A9}$$

$$\overline{M}_d = V_d \overline{C}_d = \frac{X_0 V_d}{sV_d + D_m A q_m} \tag{A10}$$

$$\overline{M}_m = \int_0^\infty (A + A'')\overline{C}_m \partial X = \frac{X_0(A + A'')}{q_m(sV_d + D_m A q_m)} \tag{A11}$$

where A' and A'' are the volume per unit length for the capillary and intracellular compartments, respectively, and the following relationships are valid.

$$r_p = \frac{A'}{A + A' + A''}, \qquad r_i = \frac{A}{A + A' + A''},$$

$$r_c = \frac{A''}{A + A' + A''} \tag{A12}$$

For ^{14}C-carbohydrates, the Laplace transforms of Eqs. (12)–(13) are, respectively,

$$s\overline{C}_m = D_m \frac{\partial^2 \overline{C}_m}{\partial X^2} - k_m \overline{C}_m + k_p(r_p/r_i)\overline{C}_p \tag{A13}$$

$$s\overline{C}_p = k_m(r_i/r_p)\overline{C}_m - (k_q + k_q)\overline{C}_p \tag{A14}$$

From Eqs. (A2)–(A4), (A13), and (A14),

$$\overline{C}_m = \frac{X_0}{sV_d + q'_m D_m A} \exp(-q'_m X) \tag{A15}$$

$$\overline{C}_p = \frac{k_m(r_i/r_p)X_0}{(s + k_p + k_q)(sV_d + q'_m D_m A)} \exp(-q'_m X) \tag{A16}$$

where

$$q'_m = \left[\frac{s^2 + (k_m + k_p + k_q)s + k_m k_q}{D_m(s + k_p + k_q)}\right]^{1/2} \tag{A17}$$

$\bar{J}_a$, $\overline{M}_d$, and $\overline{M}_m$ are calculated, respectively, as follows:

$$\bar{J}_a = \int_0^\infty k_q A' \bar{C}_p \, \partial X = \frac{k_m k_q A X_0}{q_m(sV_d + D_m A q_m)(s + k_p + k_q)} \quad \text{(A18)}$$

$$\bar{M}_d = V_d \bar{C}_d = \frac{V_d X_0}{sV_d + daq_m} \quad \text{(A19)}$$

$$\bar{M}_m = \int_0^\infty \bar{C}_m A \partial X = \frac{AX_0}{q_m(sV_d + D_m A q_m)} \quad \text{(A20)}$$

APPENDIX B: CALCULATION OF THE FIRST MOMENT (FIG. 2)

$\bar{t}_a$, $\bar{t}_d$, and $\bar{t}_m$ for each compound are calculated by the following equations (20):

$$\bar{t}_a = \lim_{s \to o} - d/ds \, [\ln \bar{J}_a] \quad \text{(A21)}$$

$$\bar{t}_x = \frac{1}{X_0} \int_0^\infty M_x(t) \, dt = \lim_{s \to o} \left[\frac{\bar{M}_x(s)}{X_0} \right] \quad (x = d \text{ or } m) \quad \text{(A22)}$$

where $M_x(t)$ is the amount of each compound in the depot or muscle at time t and $\bar{M}_x(s)$ is the Laplace transform of $M_x(t)$. Using these relationships, $\bar{t}_a$, $\bar{t}_d$, and $\bar{t}_m$ can be calculated for ^{3}H-water [Eqs. (7)–(9)] and ^{14}C-labeled carbohydrates [Eqs. (19)–(21)]. $\bar{t}_b$ values for each compound can be obtained as follows:

$$\bar{t}_b = \bar{t}_a - (\bar{t}_d + \bar{t}_m) \quad \text{(A23)}$$

ACKNOWLEDGMENT

The authors thank Professor Hitoshi Sezaki, Faculty of Pharmaceutical Sciences, Kyoto University, Kyoto, Japan, for his valuable suggestions and constructive discussion during this work.

REFERENCES

1. J. Schou. Subcutaneous and intramuscular injection of drugs. In B. B. Brodie and J. R. Gillette (eds.), *Handbook of Experimental Pharmacology, Vol. XXVIII. Concepts in Biochemical Pharmacology, Part I,* Springer-Verlag, Berlin, Heidelberg, New York, 1971, pp. 47–61.
2. B. E. Ballard. Biopharmaceutical considerations in subcutaneous and intramuscular drug administration. *J. Pharm. Sci.* 57:357–378 (1968).
3. R. E. Gosselin and G. R. Stibitz. Rate of solution absorption from tissue depots: Theoretical considerations. *Pflügers Arch.* 318:85–98 (1970).
4. P. Hildebrandt, P. Sejrsen, S. L. Nielsen, K. Birch, and L. Sestoft. Diffusion and polymerization determine the insulin absorption from subcutaneous tissue in diabetic patients. *Scand. J. Clin. Lab. Invest.* 45:685–690 (1985).
5. E. Mosekilde, K. S. Jensen, C. Binder, S. Pramming, and B. Thorsteinsson. Modeling absorption kinetics of subcutaneous injected soluble insulin. *J. Pharmacokin. Biopharm.* 17:67–87 (1989).
6. E. Nara, T. Hatono, M. Hashida, and H. Sezaki. A new method for assessment of drug absorption from muscle: Application of a local perfusion system. *J. Pharm. Pharmacol.* 43:272–274 (1991).
7. Y. Yano, K. Yamaoka, and H. Tanaka. A nonlinear least squares program, MULTI(FILT), based on fast inverse Laplace transform for microcomputers. *Chem. Pharm. Bull.* 37:1035–1038 (1989).
8. C. Crone and D. G. Levitt. Capillary permeability to small solutes. In E. M. Renkin and C. C. Michel (eds.), *Handbook of Physiology. Section 2: The Cardiovascular System, Vol. IV,* American Physiological Society, Bethesda, Md., 1984, pp. 411–466.
9. R. O. Law. Technique and application of extracellular space determination in mammalian tissue. *Experientia* 38:411–520 (1982).
10. D. J. Hnatowich, W. W. Layne, and R. L. Childs. The preparation and labeling of DTPA coupled albumin. *Int. J. Appl. Radiot. Isot.* 33:327–332 (1982).
11. T. Kakutani, K. Yamaoka, M. Hashida, and H. Sezaki. A new method for assessment of drug disposition in muscle: Application of statistical moment theory to local perfusion system. *J. Pharmacokin. Biopharm.* 13:609–631 (1985).
12. G. W. Roberts, K. B. Larson, E. E. Speath. The interpretation of mean transit time measurements for multiphase tissue systems. *J. Theor. Biol.* 39:447–475 (1973).
13. C. Crone and D. Garlick. The penetration of inulin, sucrose, mannitol and tritiated water from the interstitial space in muscle into the vascular system. *J. Physiol.* 210:387–404 (1970).
14. N. F. Paradise, C. R. Swayze, D. H. Shin, and I. J. Fox. Perfusion heterogeneity in skeletal muscle using a tritiated water. *Am. J. Physiol.* 220:1107–1115 (1971).
15. P. O. Iversen, M. Standa, and G. Nicolaysen. Marked regional heterogeneity in blood flow within a single skeletal muscle at rest and during exercise hypeaemia in the rabbit. *Acta Physiol. Scand.* 136:17–28 (1989).
16. J. L. Bert and R. H. Pearce. The interstitium and microvascular exchange. In E. M. Renkin and C. C. Michel (eds.), *Handbook of Physiology. Section 3: The Cardiovascular System, Vol IV,* American Physiological Society, Bethesda, Md., 1984, pp. 521–547.
17. R. K. Jain. Transport of molecules in the tumor interstitium: A review. *Cancer Res.* 47:3039–3051 (1987).
18. R. B. Sund and J. Schou. Hyaluronidase as an accelerator of muscular absorption of water and water soluble compounds. *Acta Pharmacol. Toxicol.* 23:194–204 (1965).
19. H. Kobayashi, T. Peng, R. Kawamura, S. Muranishi, and H. Sezaki. Mechanism of the inhibitory effect of surfactants on intramuscular absorption of drugs. *Chem. Pharm. Bull.* 25:1547–1554 (1977).
20. H. Okamoto, F. Yamashita, K. Saito, and M. Hashida. Analysis of drug penetration through the skin by the two-layer skin model. *Pharm. Res.* 6:931–937 (1989).